Electrical coupling of individual electrocatalytic oscillators

Cite as: Chaos **32**, 083139 (2022); https://doi.org/10.1063/5.0098339
Submitted: 07 May 2022 • Accepted: 28 July 2022 • Published Online: 24 August 2022

R. L. Romano, L. P. Damaceno, D. V. Magalhães, et al.

Electrical coupling of individual electrocatalytic oscillators

Cite as: Chaos **32**, 083139 (2022); doi: 10.1063/5.0098339
Submitted: 7 May 2022 · Accepted: 28 July 2022 ·
Published Online: 24 August 2022

R. L. Romano,[1] L. P. Damaceno,[2] D. V. Magalhães,[2] P. Parmananda,[3] and H. Varela[1,a)]

AFFILIATIONS

[1]São Carlos Institute of Chemistry, University of São Paulo, 13560-970 São Carlos, SP, Brazil
[2]Department of Mechanical Engineering, University of São Paulo, 13560-970 São Carlos, SP, Brazil
[3]Department of Physics, Indian Institute of Technology, Bombay, Powai, Mumbai 400076, India

Note: This article is part of the Focus Issue, From Chemical Oscillations to Applications of Nonlinear Dynamics: Dedicated to Richard J. Field on the Occasion of his 80th Birthday.
[a)]**Author to whom correspondence should be addressed:** hamiltonvarela@usp.br

ABSTRACT

The catalytic electro-oxidation of some small organic molecules is known to display kinetic instabilities, which reflect on potential and/or current oscillations. Under oscillatory conditions, those systems can be considered electrocatalytic oscillators and, therefore, can be described by their amplitude, frequency, and waveform. Just like mechanical oscillators, the electrocatalytic ones can be coupled and their dynamics can be changed by setting different coupling parameters. In the present work, we study the unidirectional coupling of electrocatalytic oscillators, namely, those comprehending the catalytic electro-oxidation of methanol and formic acid on polycrystalline platinum in acidic media under potentiostatic control. Herein, we explore two different scenarios (the coupling of compositionally identical and non-identical oscillators) and investigate the effects of the master's identity and of the coupling constant on the slave's dynamics. For the master (methanol)–slave (methanol) coupling, the oscillators exhibited phase lag synchronization and complete phase synchronization. On the other hand, for the master (formic acid)–slave (methanol) coupling, the oscillators exhibited complete phase synchronization with phase-locking with a 2:3 ratio, complete phase synchronization with phase-locking with a 1:2 ratio, phase lag synchronization, and complete phase synchronization. The obtained results suggest that both the master's identity and the coupling constant (sign and magnitude) are parameters that play an important role on the coupled systems, in such a way that even for completely different systems, synchronization could emerge by setting a suitable coupling constant. To the best of our knowledge, this is the first report concerning the electrical coupling of hidden N-shaped-negative differential resistance type systems.

The catalytic electro-oxidation of small organic molecules enables the interconversion of chemical and electrical energies on the so-called fuel cells as well as on the hydrogen production. Most of those reactions are known to display kinetic instabilities in the form of current and/or potential oscillations. Herein, we report on the unidirectional coupling of compositionally identical and non-identical electrocatalytic oscillators, namely, the electro-oxidation of formic acid and methanol on platinum, and explore how the nature of the master system affects the oscillatory dynamics of the slave in terms of its frequency, amplitude, and waveform.

INTRODUCTION

The growing interest on the catalytic electro-oxidation of small organic molecules is an immediate result of the worldwide concern on sustainability and energy demand.[1–3] Arising as reactions that enable the interconversion between chemical and electrical energies, the electrocatalytic oxidation of formic acid, methanol, or ethanol has been explored on the so-called fuel cells as well as on the hydrogen production by the electrochemical reform process. Although promising, the aforementioned systems face several practical limitations, such as catalyst poisoning by reaction intermediates and sluggish kinetics.[4–8]

It is well known that, depending on the operation conditions, kinetic instabilities can be observed during the catalytic electro-oxidation of small organic molecules, which reflect on current and/or potential oscillations.[9,10] These electrocatalytic oscillators are of the HN-NDR type since they present a partially hidden (H) negative differential resistance (NDR) in an N-shaped current vs potential curve.[11–13] The study of these nonlinearities is of great interest from a fundamental perspective since many mechanistic information has been obtained by evaluating the dynamic behavior under different experimental conditions.[14–19] Besides, the understanding of these oscillations is of extreme importance from an applied perspective: as shown by Varela and co-workers,[20,21] who studied the half-cell electro-oxidation of a set of seven organic molecules on polycrystalline platinum in acidic media, a performance improvement can be obtained while operating under an oscillatory regime.

Concerning kinetic instabilities in practical devices, an interesting finding was reported by Nogueira *et al.*,[22] who studied the time evolution of the potential of both anode and cathode of fuel cells operating under an oscillatory regime. Either using methanol or formic acid, the authors found that cathode and anode dynamics were coupled and the cathode dynamics were synchronized to that of the cell potential. In this context, to the best of our knowledge, there is no report in the current literature concerning the coupling of anodic reactions involving the electro-oxidation of small organic molecules. It is far more common to find studies concerning coupling of oscillators resulting from the electro-dissolution of metallic electrodes, for example. In general, these reports show that by coupling electrically two electrochemical/chemo-mechanical oscillators, their amplitude, frequency, and/or waveform can be changed compared to their autonomous dynamics.[23–33]

There are many electrical coupling configurations, but two special cases must be emphasized: the unidirectional and bidirectional coupling. In the first case, there is a master–slave configuration, where the master evolves freely while the slave's evolution is affected by the former's dynamics. During the bidirectional coupling, there is a mutual interaction of the oscillators so that one affects the dynamics of the other and vice versa.[34] For both cases, depending on the experimental conditions, the synchronization phenomena can be observed, which can be defined as a condition where two or more oscillators exhibit a coordinated action, adjusting a given property in such a way it evolves similarly in both systems.[34] Thus, during the coupling, different synchronized states can emerge, such as phase synchronization, lag synchronization, complete synchronization, etc.

Parmananda and co-workers[23] investigated the different domains of synchronization that could emerge during the unidirectional coupling of non-identical electrochemical oscillators. The experimental setup consisted of two separated electrochemical cells (electrolyte: 1.0 mol l^{-1} H_2SO_4, 0.4 mol l^{-1} K_2SO_4, and 53.66 mol l^{-1} KCl), connected electrically by a computer; all experiments were carried potentiostatically, with the anodic current coming from the electro-dissolution of the iron-made working electrodes. In their study, the potential applied to the master oscillator (E_m) was kept constant, while the potential applied to the slave was continually varied according to Eq. (1),

$$E_s = E_{s,i} + k(I_m - I_s), \tag{1}$$

where $E_{s,i}$ is the potential initially applied to the slave (kept constant), k is the coupling constant, I_m is the current from the master, and I_s is the current from the slave.[23] Here, k is an electrical parameter and can be understood as a measurement of the strength of the coupling: the higher the k module, the stronger the coupling.

In short, by monotonically increasing the coupling constant from 0 up to 0.12 V A^{-1}, the authors found the following synchronized states: no synchronization ($k = 0$ V A^{-1}), phase synchronization ($k = 0.012$ V A^{-1}), lag synchronization ($k = 0.025$ V A^{-1}), and complete synchronization ($k = 0.12$ V A^{-1}).[23] That is, the slave dynamics was modified during the unidirectional coupling, following the dynamics of the master.

Cruz *et al.*[24] investigated the bidirectional coupling of non-identical electrochemical oscillators. In this case, the iron-made working electrodes were inserted into the same electrolyte, into the same cell, and the distance (d) between them was a measurement of the coupling constant: the higher the distance, the weaker the coupling. All experiments were carried potentiostatically. By setting d values equal to 5, 3.5, 2.4, and 1.35 cm, the following synchronized states were observed: no synchronization, phase synchronization, lag synchronization, and complete synchronization.

As described above, both unidirectional and bidirectional coupling lead to changes on the dynamics of at least one of the oscillators, changing its amplitude, frequency, or waveform. In this sense, we believe that the electrical coupling of electrocatalytic oscillators is an alternate approach to reach greater performance in practical systems, making a less active system to be driven by a more active one. For example, the electro-oxidation of formic acid on platinum in acidic media results in higher voltammetric currents than that of methanol under identical conditions, even though complete oxidation of 1 mol of the latter results in 6 mol of electrons, while the oxidation of the former results in only 2.[35]

Thus, in the present work, we study the unidirectional coupling of compositionally identical and non-identical electrocatalytic oscillators. By using HN-NDR type systems, with methanol and formic acid as organic molecules, we investigate how the master's identity affects the oscillatory dynamics of the slave in terms of its frequency, amplitude, and waveform. Insights on the electrical coupling of anodic reactions are presented. To the best of our knowledge, coupling of HN-NDR type systems has not been explored earlier.

EXPERIMENTAL

General

Experiments were carried out in two conventional thermostated three-electrode glass cells. Polycrystalline platinum flags were used as working (0.21 and 0.28 cm^{-2} of geometric area) and counter (0.84 and 0.91 cm^{-2} of geometric area) electrodes, while a reversible hydrogen electrode prepared with 0.5 mol l^{-1} sulfuric acid was used as a reference electrode. The supporting electrolyte was a 0.5 mol l^{-1} H_2SO_4 (Merck, 96%) solution, and methanol (Qhemis, 99.8%) and formic acid (Panreac, 98%) were used at 1.0 mol l^{-1}. All solutions were prepared with high purity water (Millipore - Milli-Q System, 18 MΩ cm).

The electrochemical measurements were taken with two potentiostats AUTOLAB (PGSTAT302N and PGSTAT204), which were

controlled by the software NOVA 1.11, AUTOLAB SDK, and LabVIEW 2015 (National Instruments). Decade resistance boxes (Minipa, MDR610 and MDR611, ±0.5 Ω) were used to apply different external resistance values between the working electrode and the potentiostat.

Before starting measurements, the following procedures were adopted: (1) In each cell, argon (White Martins, 99.996%) was purged into the electrolyte for 20 min to remove dissolved oxygen. (2) The working electrodes underwent flame annealing (butane/air) and were cooled in an inert atmosphere. (3) Electrochemical annealing of the working electrodes with 250 voltammetric cycles at 200 mV s^{-1} between 0.05 and 1.40 V was performed in the supporting electrolyte. After these procedures, cyclic voltammograms of the polycrystalline platinum were recorded at 50 mV s^{-1} before and after adding methanol or formic acid.

Oscillatory dynamics under a potentiostatic regime

To estimate which potential could lead to the emergence of current oscillations for a given external resistance (R_{ext}), slow linear sweep voltammetry measurements (at 5 mV s^{-1}) were taken for R_{ext} values between 0 and 3.0 kΩ. Then, chronoamperometric measurements were performed for different combinations of applied potential and external resistance. Before each measurement, cyclic voltammetry (10 cycles, at 100 mV s^{-1}) was performed without any external resistance between the working electrode and the potentiostat.

Electrical coupling of electrocatalytic oscillators

A method similar to that described by Parmananda and coworkers[23] was used to study the unidirectional coupling of electrocatalytic oscillators. Figure 1 shows a detailed schematic of the experimental setup employed, evidencing the connections and the information shared between each component of the system.

The left branch of the schematic is related to the master oscillator: an electrochemical cell (Cell 1) is connected to a potentiostat (PGSTAT302N), which is then connected to Computer 1. In this case, the applied potential (E_m) is kept constant while the measurement is running, and the resulting current is recorded by the computer. On the other hand, the right branch is related to the slave oscillator: an electrochemical cell (Cell 2) is connected to a potentiostat (PGSTAT204), which is then connected to Computer 2. For the slave, the applied potential (E_s) is variable and modified continuously according to Eq. (1) while the measurement is running.

The use of the software AUTOLAB SDK and LabVIEW® allowed us to modulate E_s according to Eq. (1) and modify $E_{s,i}$ and the coupling constant k whenever necessary. Besides, by using an ethernet connection and by adjusting the networking settings, I_m values could be sent from Computer 1 to Computer 2. In this step, a local ethernet network had to be implemented, with one computer acting as a server and the other as a client.

In this work, the unidirectional coupling was studied by considering two different scenarios. In the first one, the coupled oscillators were compositionally identical (methanol was used as an organic molecule in both electrochemical cells), even though some electrical parameters were chosen to be different. On the other hand, in the second scenario, we modified the master's identity (methanol was replaced by formic acid) so that the coupled oscillators were not compositionally identical. From now on, the coupled systems of each scenario will be referred, respectively, as master (methanol)–slave (methanol) and master (formic acid)–slave (methanol).

Under coupling conditions, all measurements were taken potentiostatically. For the master (methanol)–slave (methanol)

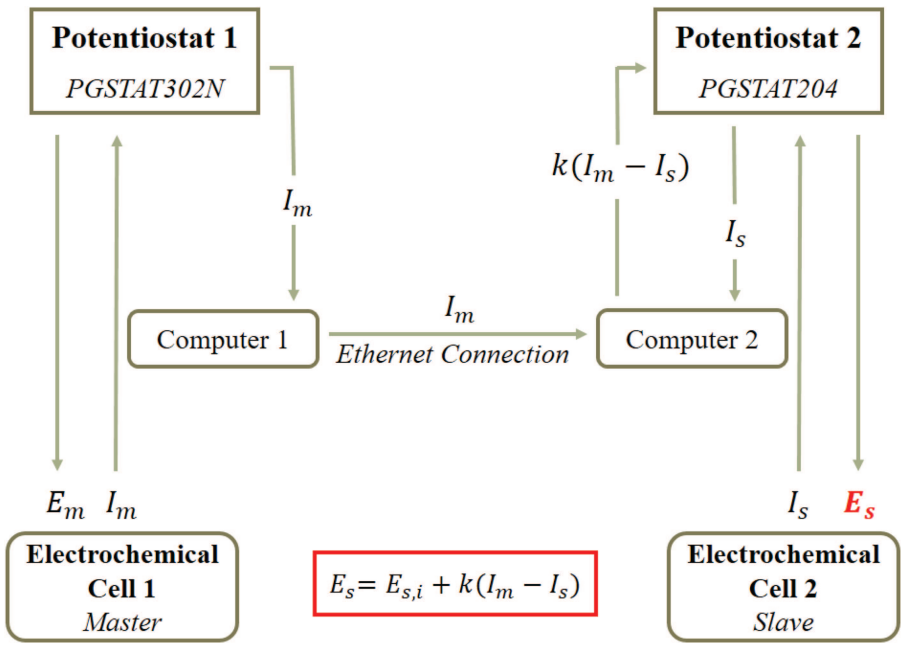

FIG. 1. Scheme of the experimental setup employed to study the unidirectional coupling of electrocatalytic oscillators. E_m is the potential applied to the master oscillator, E_s is the potential applied to the slave oscillator, $E_{s,i}$ is the potential initially applied to the slave, k is the coupling constant, I_m is the current from the master, and I_s is the current from the slave. An ethernet connection allowed the information exchange between the computers so that the potential of the slave could be modulated according to the equation highlighted in the red box.

coupling, the following parameters were chosen to the oscillators: $E_m = 1.645$ V, $E_{s,i} = 1.635$ V, and $R_{ext} = 2.0$ kΩ. On the other hand, for the master (formic acid)–slave (methanol), $E_m = 1.683$ V, $R_{ext(master)} = 1.2$ kΩ, $E_{s,i} = 1.635$ V, and $R_{ext(slave)} = 2.0$ kΩ. For both cases, the chronoamperometric measurements were performed in such a way that the master started oscillating a few seconds before the slave. Then, only when the slave started to oscillate, the coupling was initiated by setting a k value different from zero. The time evolution of the oscillators was then recorded for different coupling constant values.

RESULTS AND DISCUSSION

Oscillatory electro-oxidation of methanol and formic acid on polycrystalline platinum

The voltammetric characterization of the polycrystalline platinum electrodes in 0.5 mol l^{-1} H_2SO_4, before and after addition of methanol or formic acid, is shown in Fig. S1 of the supplementary material. The obtained voltammetric profiles are in agreement with previously published results.[36–38]

Figure 2(a) shows a representative full time-series for the potentiostatic electro-oxidation of methanol on polycrystalline platinum, with $E = 1.645$ V and $R_{ext} = 2.0$ kΩ. E and R_{ext} values were chosen based on the slow linear sweep voltammetry measurements, shown in Fig. S2 of the supplementary material. The current oscillations start at ∼0.48 mA after a short induction period and then develop between ∼0.40 and 0.55 mA. As system evolves, different oscillatory behaviors can be observed, as depicted in Figs. 2(b)–2(g).

At the beginning of the time series, period-1 oscillations emerge [Figs. 2(b) and 2(c)], which experiences waveform and amplitude changes over time. After ∼900 s, more complex dynamics emerge [Figs. 2(d)–2(g)], showing period changes and mixed mode patterns, which can be related to uncompensated oscillations.[39–41]

Figure 3(a) shows a representative full time-series for the potentiostatic electro-oxidation of formic acid on polycrystalline platinum, with E = 1.683 V and R_{ext} = 1.2 kΩ. In this case, there is no induction period and the current oscillations develop between ∼0.67 and 0.92 mA. As system evolves, waveform and amplitude changes can be observed, as evidenced in Figs. 3(b)–3(d).

The emergence of dynamic instabilities during the electro-oxidation of small organic molecules, as those shown in Figs. 2 and 3, is commonly related to the competition between reaction intermediates for active sites on the electrode surface.[9] Considering the specific case of the electro-oxidation of methanol or formic acid in aqueous acidic media on polycrystalline platinum, the main intermediates involved are adsorbed CO and adsorbed oxygenated

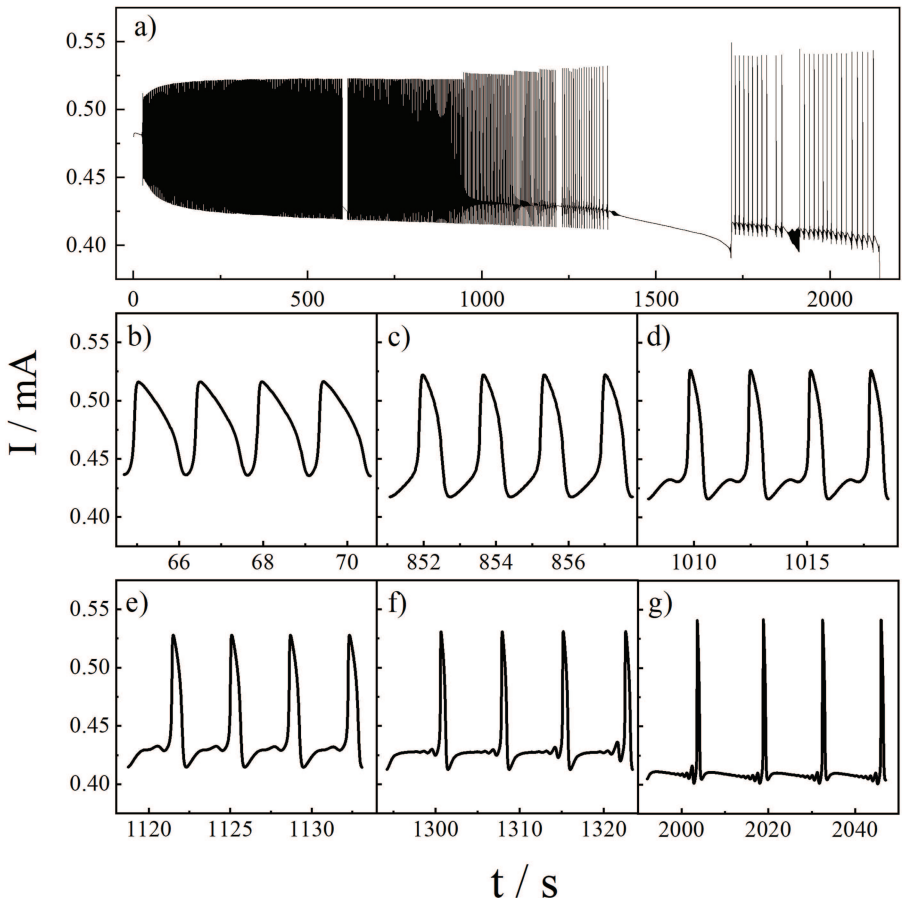

FIG. 2. (a) Full time-series for the potentiostatic electro-oxidation of methanol on polycrystalline platinum, with $E = 1.645$ V and $R_{ext} = 2.0$ kΩ. (b)–(g) Selected snapshots of the time series shown in (a), evidencing the changes in the waveform and amplitude of the current oscillations over time. [H_3COH] = 1.0 mol l^{-1}, [H_2SO_4] = 0.5 mol l^{-1}, and T = 25 °C.

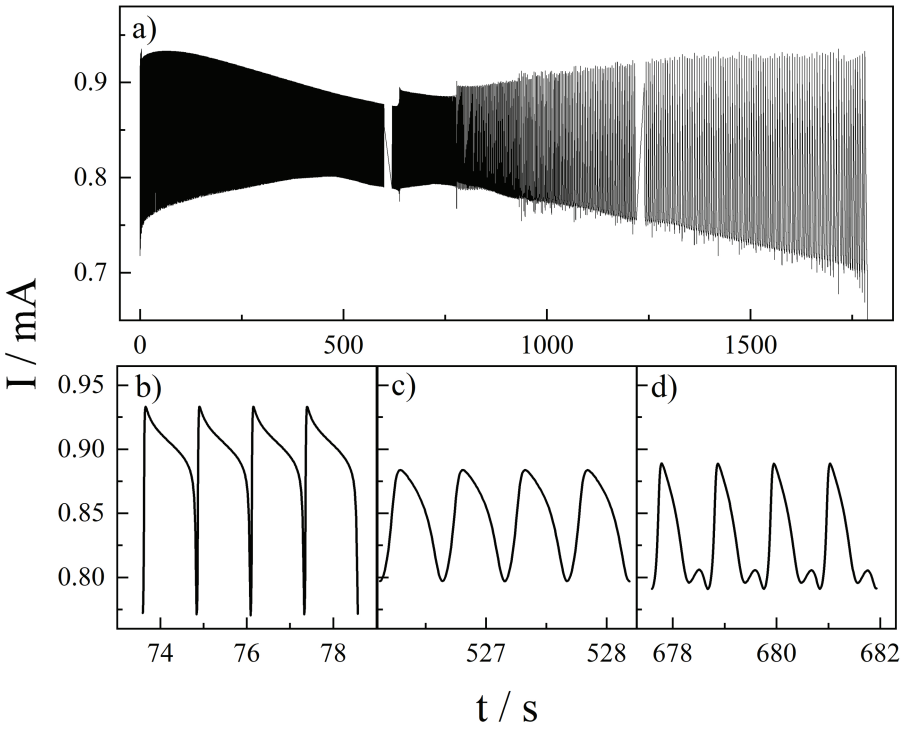

FIG. 3. (a) Full time-series for the potentiostatic electro-oxidation of formic acid on polycrystalline platinum, with $E = 1.683$ V and $R_{ext} = 1.2$ kΩ. (b)–(d) Selected snapshots of the time series shown in (a), evidencing the changes in the waveform and amplitude of the current oscillations over time. [HCOOH] = 1.0 mol l^{-1}, [H_2SO_4] = 0.5 mol l^{-1}, and T = 25 °C.

species. The former intermediate, formed in low overpotential values, adsorbs strongly on the platinum surface and blocks the active sites, leading to a current decrease. On the other hand, the adsorbed oxygenated species are formed in high overpotential values and can act as surface-blocking or can contribute to an increase of the availability of free active sites by reacting with CO_{ad} via a Langmuir–Hinshelwood mechanism resulting in CO_2 formation. Thus, depending on the experimental conditions, these competitions lead to changes in the population of the adsorbed intermediates as the electro-oxidation reaction proceeds, which can result in potential or current oscillations.[9,39]

Unidirectional coupling of electrocatalytic oscillators

As already described in the Experimental section, the unidirectional coupling was studied by considering two different scenarios. The simplest case, where compositionally identical oscillators were employed, will be presented first. Thus, for the master (methanol)–slave (methanol) coupling, an electrical parameter mismatch (different values of the initially applied potential, E_m and $E_{s,i}$) was intentionally applied: $E_m = 1.645$ V and $E_{s,i} = 1.635$ V, while $R_{ext} = 2.0$ kΩ for both oscillators. Besides, the coupling was performed, while the master oscillator was showing period-1 oscillations, such as those shown in Figs. 2(b) and 2(c). As a first approach, we investigated the effects of the sign and magnitude of the coupling constant k on the time evolution of the potential applied to the slave oscillator (E_s), as shown in Fig. 4.

Briefly, the k magnitude affects the potential window where E_s oscillates. Besides, the sign of the coupling constant also plays a role on the oscillatory behavior of E_s, but its effect becomes more evident when the magnitude of k is increased, as shown below. To gain further insight on how the sign and magnitude of the coupling constant affect the time evolution of the slave oscillator, Fig. 5 shows the time series of the potential E_s and of the anodic currents I_m and I_s for $k = 850$ V/A and −850 V/A.

As shown in Figs. 5(a) and 5(b), E_s predominantly assumes values higher than $E_{s,i} = 1.635$ V when $k < 0$, while it can assumes values higher or lower than $E_{s,i}$ when $k > 0$. This behavior can be understood by considering the relationship between I_m and I_s for each scenario [Figs. 5(c) and 5(d)]: when $k < 0$, I_s is almost always higher than I_m so that $(I_m - I_s)$ is negative. Then, considering Eq. (1), E_s will always be higher than $E_{s,i}$. However, when $k > 0$, sometimes I_s is higher than I_m, but sometimes it is not so that E_s can assumes values higher and lower than $E_{s,i}$ during the coupling.

After investigating the effects of the coupling constant on the time evolution of E_s, we sought to find k values, which could lead to the emergence of different domains of synchronization. To do so, k was monotonically increased (or decreased) from 0 to 850 V/A (or to −850 V/A). However, in contrast to previously published results, we had to interpret ours within the framework of phase synchronization. This was necessary by the extremely sensitive nature of the experimental system that made the observed dynamics quite different even for a small parameter mismatch. Specifically, since the amplitudes of the two oscillatory systems were disparate, it was decided to quantify the extent of their synchronization by the convergence of their phases. Figure 6 shows the domains of (a) no phase synchronization, characterized by the phase drift between the coupled dynamics; (b) phase lag synchronization, wherein there is

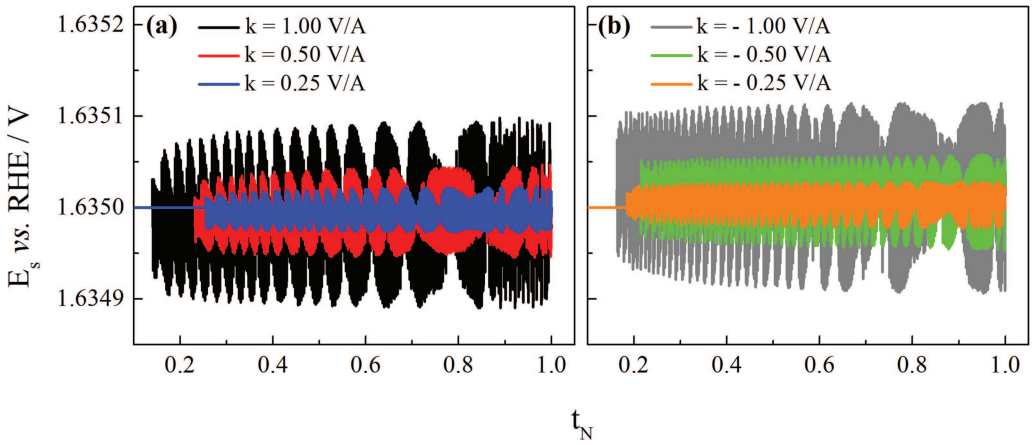

FIG. 4. Effects of the sign and magnitude of the coupling constant k on the time evolution of the potential applied to the slave oscillator (E_s) for the master (methanol)–slave (methanol) coupling, where (a) $k > 0$ and (b) $k < 0$. Time was normalized to a scale t_N, where $t_N = 0$ and $t_N = 1.0$ correspond to the beginning and end of the chronoamperometry, respectively.

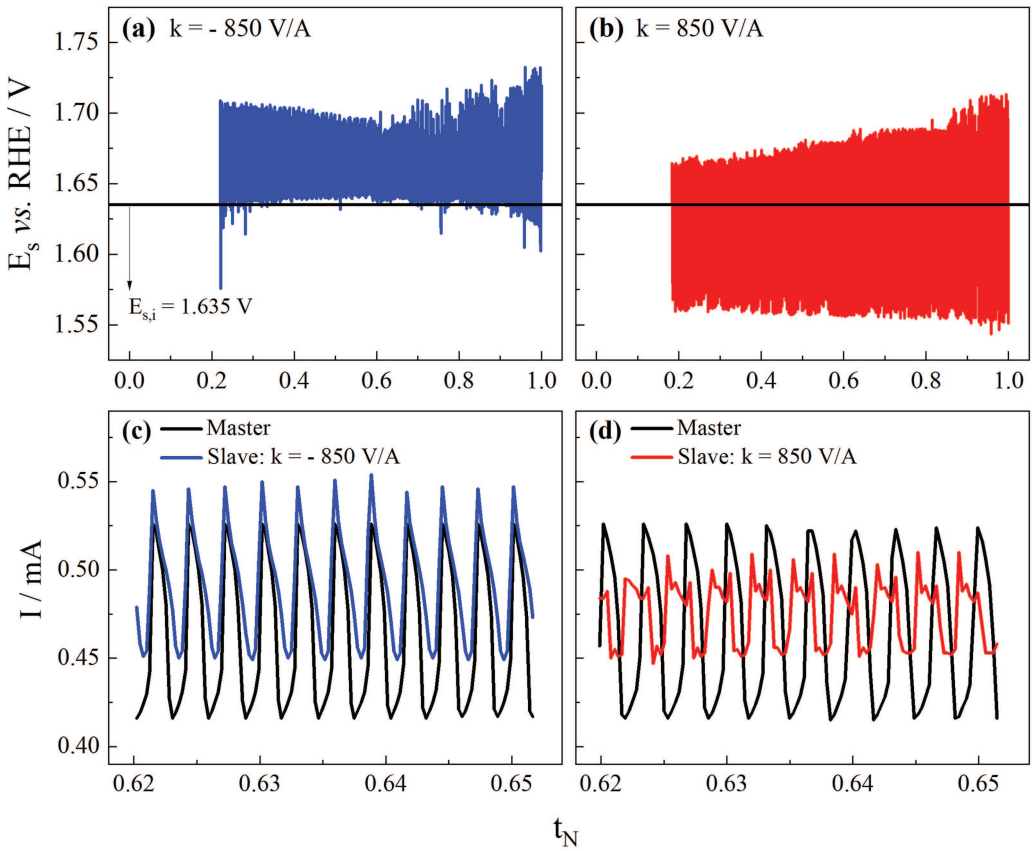

FIG. 5. Time evolution of the potential E_s for (a) $k = -850$ V/A and (b) $k = 850$ V/A. Sections of the oscillatory dynamics of the master and slave oscillators for (c) $k = -850$ V/A and (d) $k = 850$ V/A. Time was normalized to a scale t_N, where $t_N = 0$ and $t_N = 1.0$ correspond to the beginning and end of the chronoamperometry, respectively.

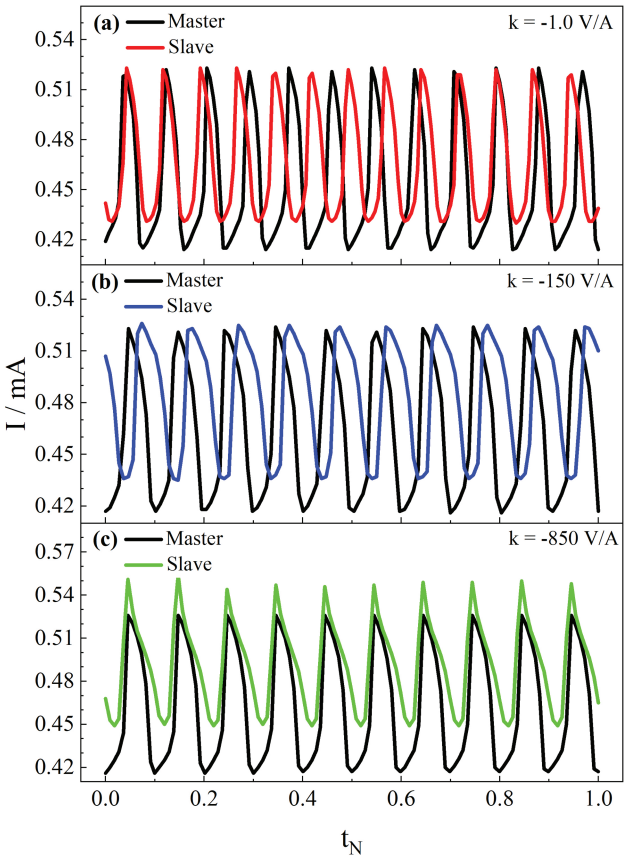

FIG. 6. Domains of synchronization identified during the unidirectional coupling of the master (methanol)–slave (methanol) system. The domains of (a) no phase synchronization (drifting phases), (b) phase lag synchronization (constant phase shift), and (c) complete phase synchronization (zero phase shift) were observed by applying k values equal to −1.0, −150, and −850 V/A, respectively.

a constant phase difference between the dynamics of the coupled oscillators (the slave lags the master); and (c) complete phase synchronization, characterized by the coincidence of the phases of the oscillators. These different domains were observed by applying k values equal to −1.0, −150, and −850 V/A, respectively. To emphasize, since the coupling was unable to achieve convergence of the amplitudes, it was decided to study the convergence of the slave dynamics within the framework of phase synchronization.

To reiterate, by increasing the coupling strength (increasing k module), the dynamics of the slave became similar to that of the master, even though it does not become identical. This is to be expected since the uncoupled dynamics of the two oscillators are extremely different. When the coupling constant is too small ($k = -1.0\ \mathrm{V\,A^{-1}}$), the coupling strength is weak and the phase of the two oscillators does not synchronize (the dynamics are drifting). On the other hand, by applying an intermediate coupling strength ($k = -150\ \mathrm{V\,A^{-1}}$), a time lag approximately constant (~0.33 s) was observed between the dynamics, which can be classified as phase lag synchronization. Finally, by applying a high coupling strength ($k = -850\ \mathrm{V\,A^{-1}}$), complete phase synchronization was identified. For the master (methanol)–slave (methanol), only negative k values led to synchronized states and the behavior shown in Figs. 6(b) and 6(c) stands during almost all the time series, featuring a stable system.

Comparing these results to that obtained by Parmananda and co-workers[23] for chaotic oscillators, where the slave dynamics become identical to that of the master at high coupling strength, suggests that the chaotic current oscillations resulting from the electro-dissolution of the iron-made working electrodes can be modulated more easily than the periodic ones resulting from the electro-oxidation of methanol. Furthermore, it is well established that the synchronization of chaotic dynamics is easier to achieve than for their periodic counterparts. This can be attributed to the fact that the chaotic dynamics have broadband frequency spectra rendering the chaotic behavior more tunable and adaptive in comparison with their periodic counterparts. This enables chaotic synchronization simpler to achieve.

It is worth emphasizing that a given synchronized state is not restricted to only one k value. Indeed, there is an interval of k values, which depends on the nature of the coupling as well as on the identity of the oscillators. For the master (methanol)–slave (methanol), for example, phase lag synchronization and complete phase synchronization were also observed for k values, which are equal to -300 and $-500\ \mathrm{V\,A^{-1}}$, respectively.

A similar approach was applied to study the master (formic acid)–slave (methanol) coupling, where non-identical oscillators were considered. First, the effects of the sign and magnitude of the coupling constant k on the time evolution of the potential applied to the slave oscillator (E_s) were investigated, and results are shown in Figs. S3 and S4 of the supplementary material. In short, E_s oscillates overtime, and it always assumes values higher and lower than $E_{s,i}$ when $k > 0$ and $k < 0$, respectively. Besides, the magnitude of k only affects how far from $E_{s,i}$ the potential E_s is (Fig. S3 in the supplementary material). This behavior is understood by considering Fig. S4 in the supplementary material, which shows that I_m is always higher than I_s (at least, for $-300 \le k \le 300\ \mathrm{V\,A^{-1}}$). Thus, $(I_m - I_s)$ is always positive, and the sign of $k(I_m - I_s)$ depends on the sign of the coupling constant.

To identify different domains of synchronization, k was increased (or decreased) from 0 to 850 V/A (or to −850 V/A). Figure 7 shows the domains of (a) complete phase synchronization with phase-locking with a 2:3 ratio, (b) complete phase synchronization with phase-locking with a 1:2 ratio, (c) phase lag synchronization, and (d) complete phase synchronization, observed when k is set to be 150, 500, −500, and −850 V/A, respectively. In this case, since the dynamics of the oscillators do not develop in a common current range, we choose to show the oscillations of the potential φ, which corresponds to the electrode potential and can be described by the following equation [Eq. (2)]:

$$\varphi = E - R_{ext} I, \tag{2}$$

where E is the applied potential (E_m or $E_{s,i}$), R_{ext} is the external resistance, and I is the anodic current.

When k is set to be $150\ \mathrm{V\,A^{-1}}$, although amplitude and waveform are completely different, a phase correlation between the

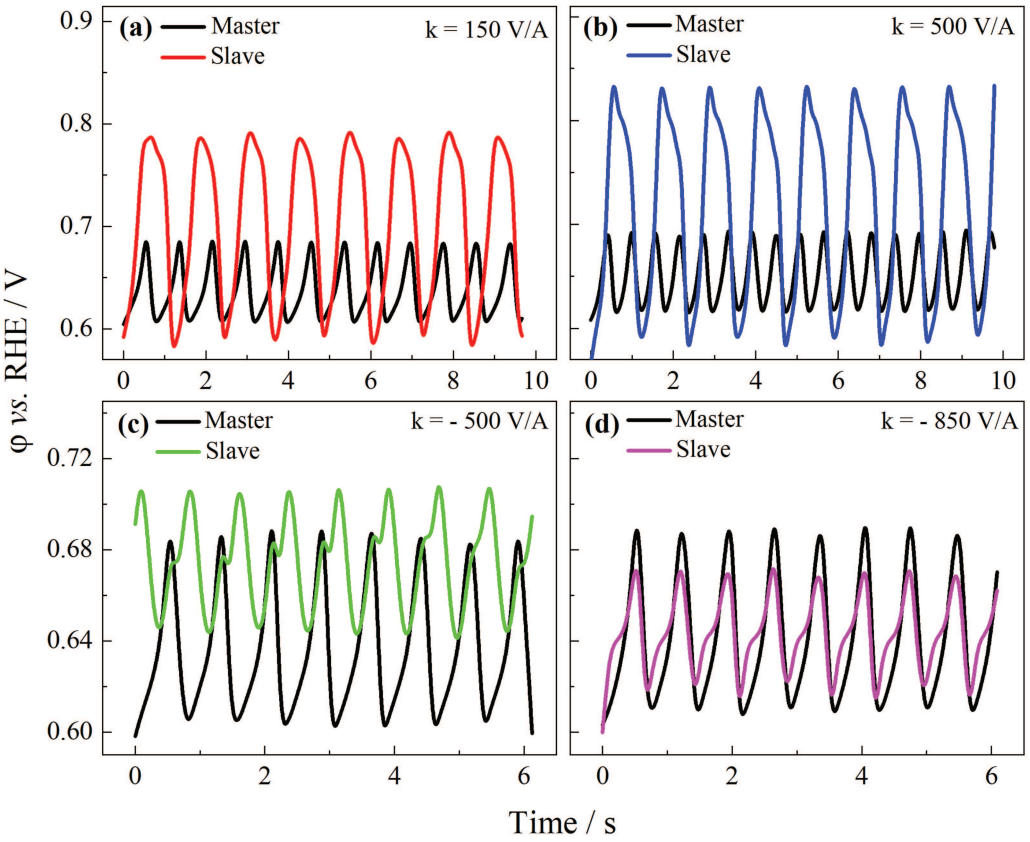

FIG. 7. Domains of synchronization identified during the electrical coupling of the master (formic acid)–slave (methanol) system. The domains of (a) complete phase synchronization with phase-locking with a 2:3 ratio, (b) complete phase synchronization with phase-locking with a 1:2 ratio, (c) phase lag synchronization, and (d) complete phase synchronization are observed when k is set to be 150, 500, −500, and −850 V/A, respectively.

dynamics is observed: for each three oscillatory cycles of the master, and there are two of the slaves, which features phase-locking with a 2:3 ratio (slave:master). Similarly, when k is set to be 500 V A^{-1}, phase-locking is observed, but with a 1:2 ratio. The observed 2:3 and 1:2 phase synchronization corresponds to the phase locked domains of the Arnold tongue commonly seen when two oscillators are configured to study the entrainment (unidirectional coupling) phenomena.

On the other hand, when $k = -500$ V A^{-1}, a time lag (~0.22 s) between the dynamics is observed, which corresponds to phase lag synchronization. Finally, when $k = -850$ V A^{-1}, complete phase synchronization was identified. To reiterate, the potential φ defined in Eq. (2) was chosen as the observable as it clearly shows the coordinated activity by virtue of the underlying unidirectional coupling between the two different oscillators.

For the master (formic acid)–slave (methanol), complete different behavior concerning the correlation between k and the observed synchronized states was found: in this case, both positive and negative k values lead to the emergence of synchronization. For the master (methanol)–slave (methanol), only negative k values allowed the emergence synchronization.

CONCLUSIONS

In the present work, we studied the unidirectional coupling of compositionally identical and non-identical electrocatalytic oscillators. By modifying the master's identity and the coupling strength, it was possible to induce changes on the oscillatory dynamics of the slave and reach different synchronized states. After synchronization, the coupled dynamics were shown to be stable, with the phase-locking standing during almost all the time series. To the best of our knowledge, this is the first report concerning the electrical coupling of HN-NDR type systems comprehending the catalytic electro-oxidation of methanol and formic acid on polycrystalline platinum in acidic media under potentiostatic control.

The coupling of two compositionally identical oscillators [master (methanol)–slave (methanol)] led to the emergence of two synchronized states as the coupling constant k was modified: both phase lag synchronization and complete phase synchronization were identified. On the other hand, for the master (formic acid)–slave (methanol) coupling, the oscillators exhibited complete phase synchronization with phase-locking with a 2:3 ratio, complete phase synchronization with phase-locking with a 1:2 ratio, phase lag synchronization, and complete phase synchronization as k was varied.

These results suggest that both the master's identity and the coupling constant (sign and magnitude) play an important role on the coupled systems in such a way that even for completely different systems, synchronization could emerge by setting a suitable coupling constant. On the other hand, our findings evidence the difficulties to modulate some periodic oscillations since the slave dynamics never got identical to that of the master (regardless of the coupling constant), even though synchronization could be achieved.

In summary, the results presented herein open perspectives to the study of the electrical coupling of other HN-NDR type systems, such as those comprehending the catalytic electro-oxidation of ethanol, formaldehyde, or even glucose, which can be done on substrates other than platinum. Additionally, the coupling configuration should not be restricted to the unidirectional one. Finally, our findings open view to an alternate approach to reach greater performance in practical systems, making a less active system to be driven by a more active one.

SUPPLEMENTARY MATERIAL

See the supplementary material for a more detailed view of the voltammetric and oscillatory behavior of the electro-oxidation of methanol and formic acid on polycrystalline platinum in acidic media and an in-depth study of the effects of the coupling constant on the master (formic acid)–slave (methanol) coupling.

ACKNOWLEDGMENTS

R.L.R. and H.V. acknowledge the São Paulo Research Foundation (FAPESP) for the scholarships (Grant No. 2018/23942-5) and financial support (No. 2019/22183-6), respectively. H.V. also acknowledges the Conselho Nacional de Desenvolvimento Científico e Tecnológico (CNPq) for financial support (No. 306060/2017-5). This study was financed in part by the Coordenação de Aperfeiçoamento de Pessoal de Nível Superior—Brasil (CAPES)—Finance Code 001.

AUTHOR DECLARATIONS

Conflict of Interest

The authors have no conflicts to disclose.

Author Contributions

R. L. Romano: Conceptualization (equal); Data curation (lead); Formal analysis (lead); Writing – original draft (lead); Writing – review & editing (equal). **L. P. Damaceno:** Methodology (equal); Software (equal). **D. V. Magalhães:** Methodology (equal); Software (equal). **P. Parmananda:** Conceptualization (equal); Writing – review & editing (equal). **H. Varela:** Conceptualization (equal); Funding acquisition (lead); Supervision (lead); Writing – review & editing (equal).

DATA AVAILABILITY

The data that support the findings of this study are available from the corresponding author upon reasonable request.

REFERENCES

[1]P. Joghee, J. N. Malik, S. Pylypenko, and R. O'Hayre, MRS Energy Sustain. **2**, 3 (2015).
[2]F. Vigier, S. Rousseau, C. Coutanceau, J. M. Leger, and C. Lamy, Top. Catal. **40**, 111 (2006).
[3]R. Schlögl, ChemSusChem **3**, 209 (2010).
[4]C. Lamy, A. Lima, V. LeRhun, F. Delime, C. Coutanceau, and J. M. Léger, J. Power Sources **105**, 283 (2002).
[5]B. C. Ong, S. K. Kamarudin, and S. Basri, Int. J. Hydrog. Energy **42**, 10142 (2017).
[6]T. Hou, S. Zhang, Y. Chen, D. Wang, and W. Cai, Renew. Sustain. Energy Rev. **44**, 132 (2015).
[7]F. M. Sapountzi, M. N. Tsampas, H. O. A. Fredriksson, J. M. Gracia, and J. W. Niemantsverdriet, Int. J. Hydrog. Energy **42**, 10762 (2017).
[8]I. Staffell, D. Scamman, A. Velazquez Abad, P. Balcombe, P. E. Dodds, P. Ekins, N. Shah, and K. R. Ward, Energy Environ. Sci. **12**, 463 (2019).
[9]H. Varela, M. V. F. Delmonde, and A. A. Zülke, *Electrocatalysts for Low Temperature Fuel Cells: Fundamentals and Recent Trends* (Wiley-VCH, 2017), pp. 145–163.
[10]K. Krischer and H. Varela, *Handbook of Fuel Cells* (John Wiley & Sons, 2010).
[11]P. Strasser, M. Eiswirth, and M. T. M. Koper, J. Electroanal. Chem. **478**, 50 (1999).
[12]T. Gojuki, Y. Numata, Y. Mukouyama, and H. Okamoto, Electrochim. Acta **129**, 142 (2014).
[13]Y. Mukouyama, S. Yamaguchi, K. Iida, T. Kuge, M. Kikuchi, and S. Nakanishi, ECS Trans. **80**, 1471 (2017).
[14]R. Nagao, D. A. Cantane, F. H. B. Lima, and H. Varela, Phys. Chem. Chem. Phys. **14**, 8294 (2012).
[15]A. Calderón-Cárdenas, F. W. Hartl, J. A. C. Gallas, and H. Varela, Catal. Today **359**, 90 (2021).
[16]H. Okamoto, N. Tanaka, and M. Naito, J. Phys. Chem. A **101**, 8480 (1997).
[17]P. Strasser, M. Lübke, F. Raspel, M. Eiswirth, and G. Ertl, J. Chem. Phys. **107**, 979 (1997).
[18]M. T. M. Koper and J. H. Sluyters, J. Electroanal. Chem. **371**, 149 (1994).
[19]D. Mei, Z. Da He, D. C. Jiang, J. Cai, and Y. X. Chen, J. Phys. Chem. C **118**, 6335 (2014).
[20]M. V. F. Delmonde, L. F. Sallum, N. Perini, E. R. Gonzalez, R. Schlögl, and H. Varela, J. Phys. Chem. C **120**, 22365 (2016).
[21]G. B. Melle, T. Altair, R. L. Romano, and H. Varela, Energy Fuels **35**, 6202 (2021).
[22]J. A. Nogueira, K. Krischer, and H. Varela, ChemPhysChem **20**, 3081 (2019).
[23]J. M. Cruz, M. Rivera, and P. Parmananda, J. Phys. Chem. A **113**, 9051 (2009).
[24]J. M. Cruz, M. Rivera, and P. Parmananda, Phys. Rev. E **75**, 035201(R) (2007).
[25]S. Fukushima, S. Nakanishi, K. Fukami, S. I. Sakai, T. Nagai, T. Tada, and Y. Nakato, Electrochem. Commun. **7**, 411 (2005).
[26]P. Kumar, D. K. Verma, P. Parmananda, and S. Boccaletti, Phys. Rev. E **91**, 062909 (2015).
[27]S. Tajima, H. Singh, S. Nakabayashi, T. Singla, and P. Parmananda, J. Electroanal. Chem. **769**, 16 (2016).
[28]D. K. Verma, H. Singh, A. Q. Contractor, and P. Parmananda, J. Phys. Chem. A **118**, 4647 (2014).
[29]D. K. Verma, H. Singh, P. Parmananda, A. Q. Contractor, and M. Rivera, Chaos **25**, 064609 (2015).
[30]D. A. Crespo-Yapur, A. Bonnefont, R. Schuster, K. Krischer, and E. R. Savinova, ChemElectroChem **1**, 1046 (2014).
[31]A. Karantonis, Y. Miyakita, and S. Nakabayashi, Phys. Rev. E **65**, 046213 (2002).
[32]A. Karantonis, M. Pagitsas, Y. Miyakita, and S. Nakabayashi, J. Phys. Chem. B **108**, 5836 (2004).
[33]J. P. Guerrette, S. M. Oja, and B. Zhang, Anal. Chem. **84**, 1609 (2012).
[34]S. Boccaletti, J. Kurths, G. Osipov, D. L. Valladares, and C. S. Zhou, Phys. Rep. **366**, 1 (2002).
[35]F. W. Hartl, A. A. Zülke, B. J. Fonte, and H. Varela, J. Electroanal. Chem. **800**, 99 (2017).

[36]M. Lukaszewski, M. Soszko, and A. Czerwiński, Int. J. Electrochem. Sci. **11**, 4442 (2016).
[37]E. Sitta and H. Varela, J. Solid State Electrochem. **12**, 559 (2008).
[38]H. Okamoto, W. Kon, and Y. Mukouyama, J. Phys. Chem. B **108**, 4432 (2004).
[39]M. F. Cabral, R. Nagao, E. Sitta, M. Eiswirth, and H. Varela, Phys. Chem. Chem. Phys. **15**, 1437 (2013).
[40]R. Nagao, E. Sitta, and H. Varela, J. Phys. Chem. C **114**, 22262 (2010).
[41]E. Boscheto, B. C. Batista, R. B. Lima, and H. Varela, J. Electroanal. Chem. **642**, 17 (2010).